Mechanical Engineering Advances 2024, 2(1), 1214.
https://doi.org/10.59400/mea.v2i1.1214

Article

Simulations of the operation of the fast light innovative regional train from "Serbian Railways" in traction and electric braking mode

Branislav Gavrilovic[1,*], Vladimir Aleksandrovich Baboshin[2]

[1] Department: Railway College, Academy of Technical and Art Applied Studies Belgrade, Zdravka Celara 14, 11000 Belgrade, Serbia
[2] Department of Reconstruction of Automation, Telemechanics and Communication Devices on Railways, Military Institute (Railway Troops and Military Communications), 190000 Sankt Peterburg, Russia
*** Corresponding author:** Branislav Gavrilovic, gavrilovicbranislav5@gmail.com

CITATION

Gavrilovic B, Baboshin VA. Simulations of the operation of the fast light innovative regional train from "Serbian Railways" in traction and electric braking mode. Mechanical Engineering Advances. 2024; 2(1): 1214. https://doi.org/10.59400/mea.v2i1.1214

ARTICLE INFO

Received: 25 August 2023
Accepted: 30 October 2023
Available online: 25 November 2023

Abstract: In the paper, the MATLAB-Simulink model of simulation of operation of the fast light innovative regional train from "Serbian Railways" in traction and braking mode is exposed where changes are observed: stator currents of three-phase traction motors, traction electric motor speeds and electric multiple units, electromagnetic torque on the rotor shaft of the traction electric motor, and direct current bus voltage. The model allowed review of the listed parameters for: different allowed values of contact network voltage and total voltage distortion at the place of connection of the electric multiple unit to the contact network; different mechanical loads of the electric multiple unit and traction electric motor; and different train speeds and rotations of traction electric motors. Appropriate conclusions were made through the analysis of the simulation results obtained.

Keywords: simulations; electric multiple unit; Serbian Railways

1. Introduction

The fast, light, innovative regional train "Serbian Railways" is a low-floor, four-part passenger train of "Serbian Railways" manufactured by the Swiss company Stadler (Company: Stadler Bussnang AG, Ernst-Stadler-Strasse 4, 9565 Bussnang, Schweiz). This fast, light, innovative regional train (FLIRT) is a specially designed electric multiple unit (EMU) of the latest generation, "FLIRT 3". At the beginning of 2014, twenty-one "FLIRT 3" were put into operation on the electric tracks of "Serbian Railways", and the procurement of thirty-one more is in progress (**Figure 1**) [1].

Figure 1. The fast, light, innovative regional train—FLIRT 3.

Basic technical data of the fast, light, innovative regional train "FLIRT 3" are shown in **Table 1** [1].

Table 1. Technical data.

Track gauge	1435 mm
Max velocity	160 km/h
Axle arrangement	Bo' 2' 2' 2' Bo'
Traction mode:	25 kV AC, 560 Hz
Maximum power on the wheel	1540 kW
Maximum starting tractive force	160 kN
Traction transformer—Main data	
Marked power	605 kVA
Maximum power per traction winding	500 kVA
Nominal voltage of traction windings	Approx. 25 kV/500 V and no load
Traction converter—Line inverter—AFE	
Input voltage	Approx. 500 VAC
Maximum input current	Approx. 1020 per AFE (2040 total)
Nominal DC-link	950 V (Under 1000 V)
Maximum output power	Approx. 525 per AFE (1050 total)
Bus capacity	85 mF
Train wide AFE synchronization	6 converters—3 EMU in multiple traction
Motor inverter—Traction three phase inverter	
Power in traction	385 kW (at wheel)
Output voltage traction	20 Hz to 120 Hz approx. from 211 V to 630 V 120 Hz to 215.7 Hz approx. 675V
Output maximum current	Approx. 780 Hz (700 Hz switching frequency)
Traction motor data	
Traction motor are three-phase asynchronous motors type	TMF 54-32-4
Continuous power	300 kW
Transmission ratio	1:5.9714

The traction equipment of the fast, light, innovative regional train "FLIRT 3" consists of:

- One pantograph for 25 kV AC.
- One traction transformer.
- Two power converters and four traction motors (2 traction motors per one power converter).
- Single-axle drive with three-phase asynchronous motors.

The traction motor is installed in the motor bogie. Wheelset axle shaft, traction motor, tooth coupling, and the gearbox together form an axle drive. There are two axle drives per motorbike. The traction motor transmits the torque to the gearbox through the tooth coupling transmission ratio of 1:5.9714. The gearbox transmits the drive torque through the wheelset axle shaft to the wheels and the tracks [1].

The traction system of the train is shown in **Figure 2**.

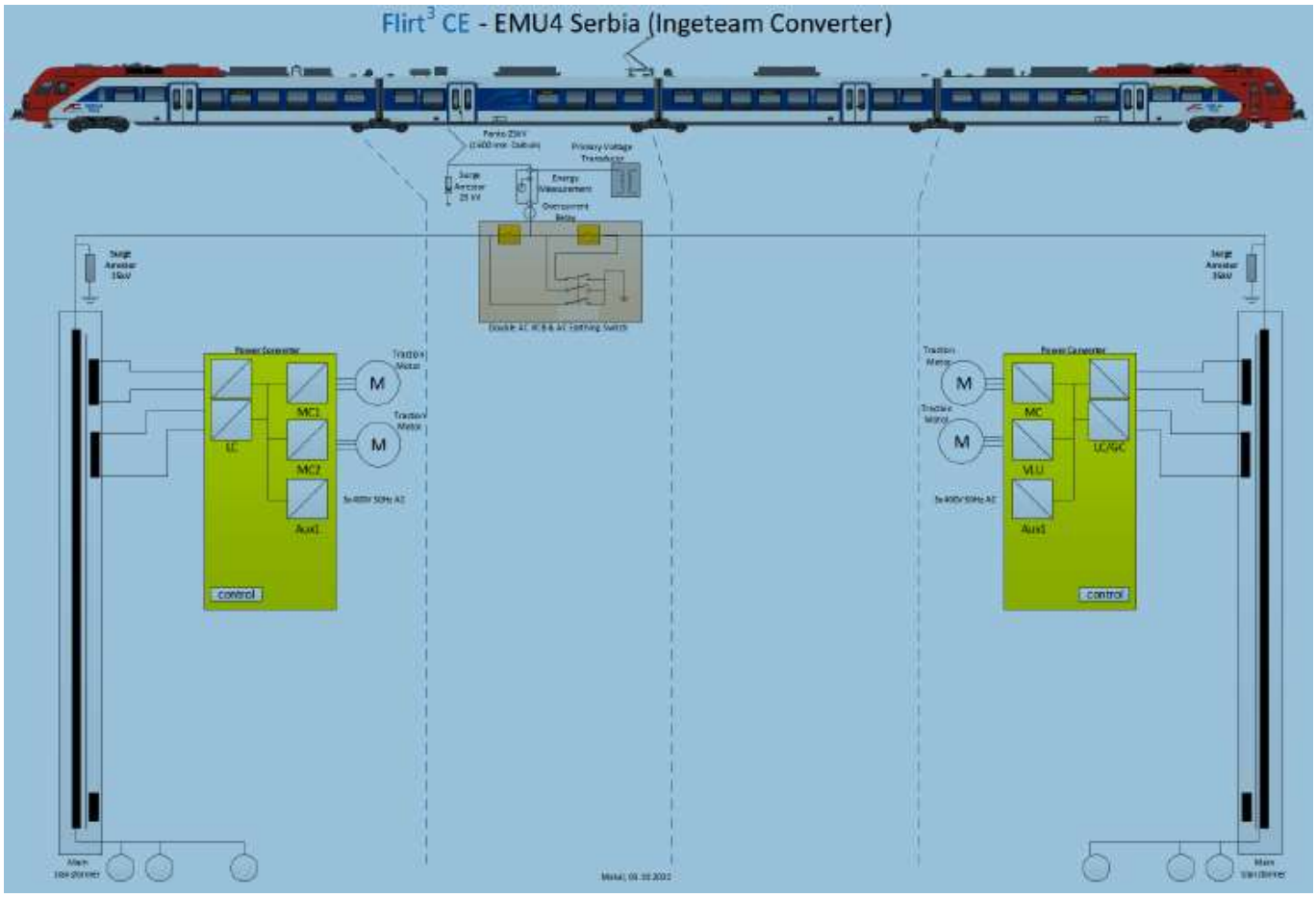

Figure 2. Principle circuit diagram main current of "FLIRT 3".

Figure 3 shows the tractive force-speed characteristics of the fast, light, innovative regional train "FLIRT 3" [1,2].

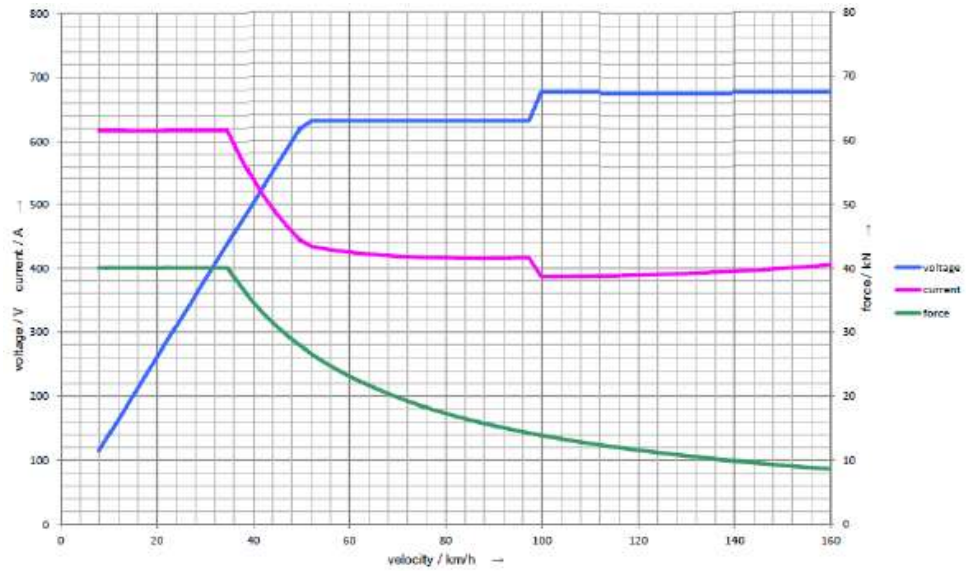

Figure 3. Traction force characteristic.

Figure 4 shows the power dependent on the line voltage of the fast, light, innovative regional train "FLIRT 3".

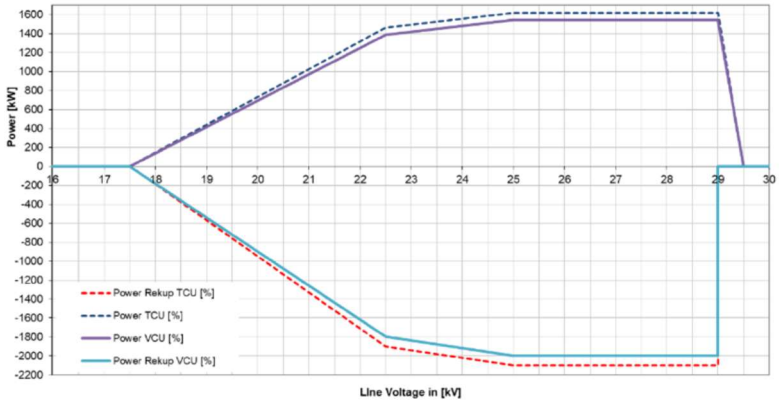

Figure 4. Power dependent on the line voltage.

2. Modeling "FLIRT 3" in MATLAB-Simulink

Modeling of the fast, light, innovative regional train "FLIRT 3" shown in MATLAB-Simulink is shown in the **Figure 5**.

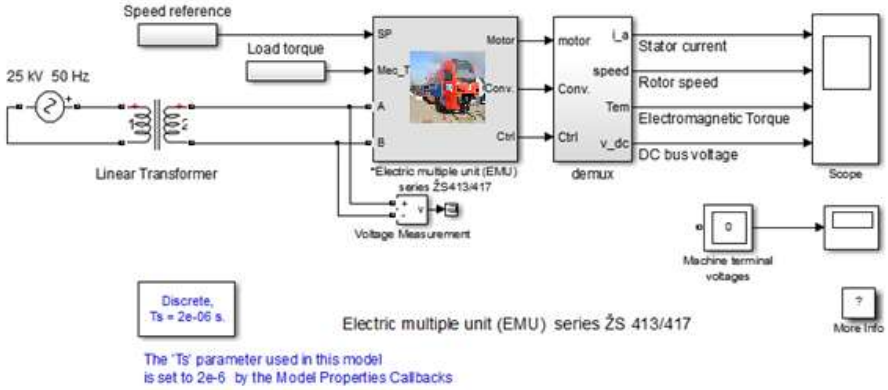

Figure 5. Simulink model of the fast, light, innovative regional train "FLIRT 3".

The high level block of the fast, light, innovative regional train "FLIRT 3" schematic shown below is built from six main blocks (**Figures 6** and **7**). The traction transformer, the induction motor, the three-phase inverter, and the mono-phase diode rectifier models are provided with the SimPowerSystems™ library. The speed controller, the braking chopper, and the DTC controller models are specific to the drive library.

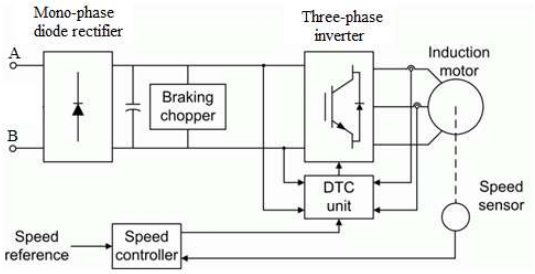

Figure 6. The high level block schematic of "FLIRT 3".

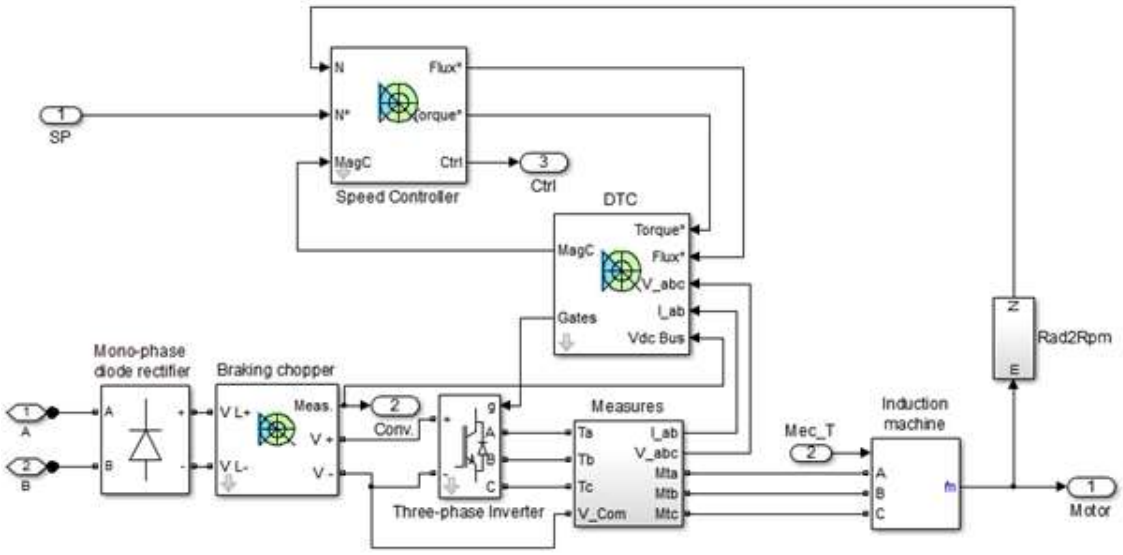

Figure 7. Simulink schematic of the fast, light, innovative regional train "FLIRT 3".

2.1. Speed controller

The speed controller is based on a PI regulator, shown below. The output of this regulator is a torque set point applied to the DTC controller block [3–15].

The high-level block diagram as well as the Simulink model of the speed controller are shown in **Figures 8** and **9** [3–15].

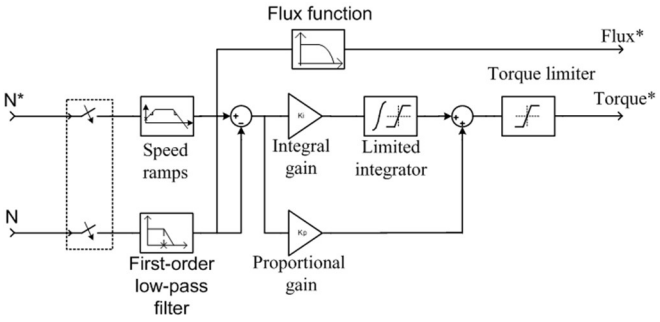

Figure 8. The high level block schematic of speed controller.

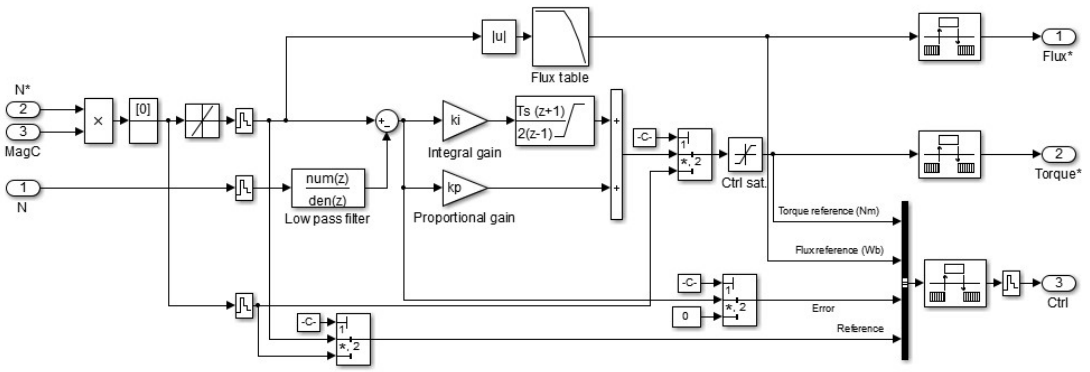

Figure 9. Simulink model of speed controller.

2.2. Braking chopper

The braking chopper block contains the DC bus capacitor and the dynamic

braking chopper, which is used to absorb the energy produced by a motor deceleration. The Simulink model of braking chopper is shown in **Figure 10** [3–15].

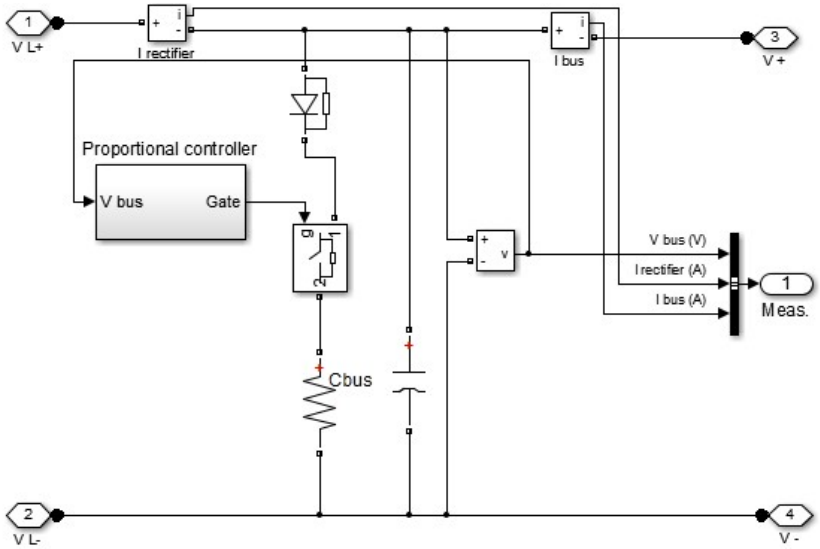

Figure 10. Simulink model of braking chopper.

2.3. DTC controller

The direct torque and flow control (DTC) controller contains five main blocks, shown in **Figure 11** [3–5].

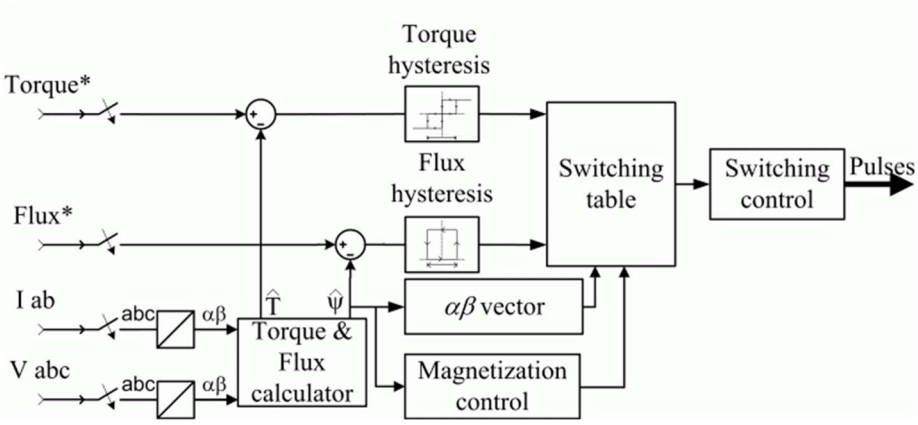

Figure 11. The direct torque and flow control (DTC) controller.

The torque & flux calculator block is used to estimate the motor flux $\alpha\beta$ components and the electromagnetic torque. This calculator is based on motor equation synthesis.

The $\alpha\beta$ vector block is used to find the sector of the $\alpha\beta$ plane in which the flux vector lies. The $\alpha\beta$ plane is divided into six different sectors spaced by 60 degrees.

The flux and torque hysteresis blocks contain a two-level hysteresis comparator for flux control and a three-level hysteresis comparator for torque control. The description of the hysteresis comparators is available below.

The switching table block contains two lookup tables that select a specific voltage vector in accordance with the output of the Flux & Torque Hysteresis comparators. This block also produces the initial flux in the machine.

The switching control block is used to limit the inverter commutation frequency to a maximum value specified by the user.

The high-level block diagram as well as the Simulink model of direct torque and flux control of the drive induction motor are shown in **Figures 11** and **12** [3–15].

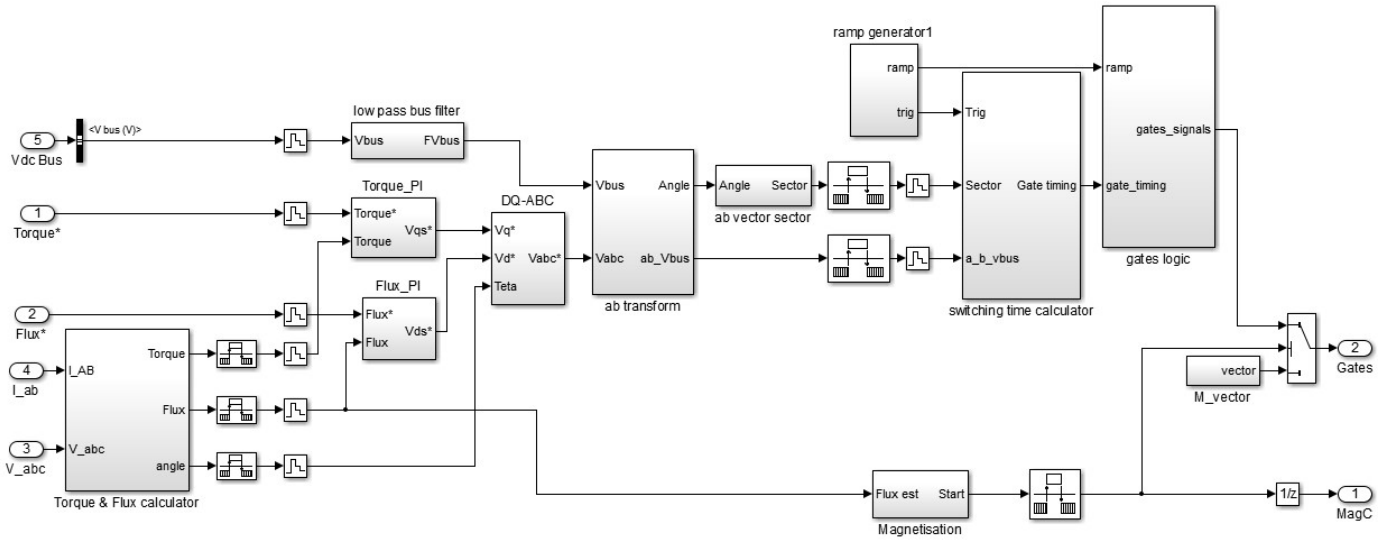

Figure 12. Simulink model of DTC (direct torque and flux control) of the drive induction motor.

2.4. Measurements

In this model, the voltage of the contact network at the connection point of the fast, light, innovative regional train "FLIRT 3" is taken as an input variable electrical quantity. This voltage can be changed within the limits of 17.5–27.5 kV according to the provisions of EN 50163. All other parameters of the Simulink model blocks are determined by the technical data of the train's devices and equipment. Electrical quantities that are measured during dynamic processes are: the stator current of the traction electric motor and the DC bus voltage converter.

The given input mechanical parameters of the model are: the desired final speed of rotation of the rotor of the traction electric motor (ω_r) and the resistive torque of the train movement (T_m). Mechanical quantities that are measured during dynamic processes and achieving the desired rotation speed are: the reverse electromagnetic torque of the traction electric motor (T_e) and the change in the rotation speed of the rotor of the traction electric motor (ω_r).

When calculating the reverse electromagnetic moment on the shaft of the traction electric motor (T_e), the equation of the dynamic balance of the train drive train was used [16–22].

$$T_e = J\frac{d}{dt}\omega_r + F\omega_r + T_m \quad (1)$$

wherein:

ω_r—speed of rotation of the rotor of the electric motor,

J—the moment of inertia of all rotating masses reduced to the rotor side of the electric motor,

F—coefficient of viscous friction,

T_m—resistance moments of movement reduced to the rotor side of the electric

motor.

By measuring and knowing the value of the reverse electromagnetic torque of the traction electric motor (T_e) and the change in the rotation speed of the rotor of the traction electric motor (ω_r), the traction force between the wheel and the rail (F_v), i.e., the translational speed of the train (v), is fully determined. The relationship between the rotating electromagnetic torque of the traction electric motor (T_e) and the traction force (F_v), i.e., the rotation speed of the rotor of the traction electric motor (ω_r) and the translation speed of the train (v), is given by the following Equation [2]:

$$F_v = \frac{2 \cdot i \cdot \eta}{D} \cdot T_e \; F_v = \frac{2i\eta}{D} T_e \tag{2}$$

$$v = \frac{D}{2i} \omega_r \tag{3}$$

wherein:

i—transmission ratio of the reducer (5.9714),

η—degree of utilization of the reducer (0.94),

D—the diameter of monobloc wheel (new/worn: 760/690 mm),

In order to monitor the change in stator current, rotation speed, and electromagnetic torque of the drive motor as well as DC bus voltage, a Simulink measurement block was modeled as in **Figure 13**.

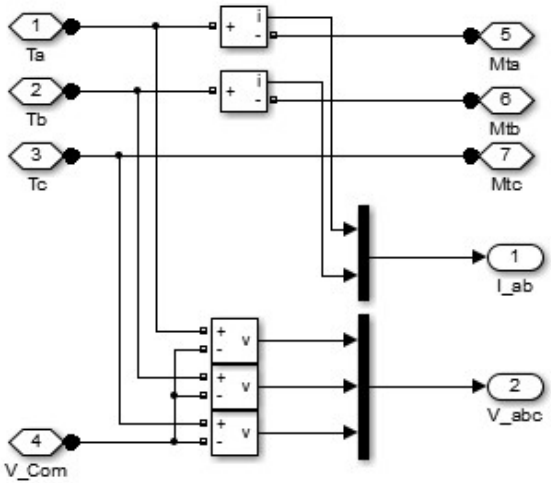

Figure 13. Simulink model of measures.

3. Results of simulations

Assuming that the given conditions are such that the fast, light, innovative regional train "FLIRT 3".

- supplies with a stable sinusoidal voltage of 25 kV, 50 Hz,
- starts from rest at time t = 0 s: up to the speed of rotation of the electric motor (v = 90 km/h),
- load so that the resistance torque on the electric motor shaft is 792 Nm in an interval 0.5–1.5, and after 1.5 s it is equal to −792 Nm,
- starts braking from the moment t = 1 s. and so on.

The simulation results are given in **Figure 14**.

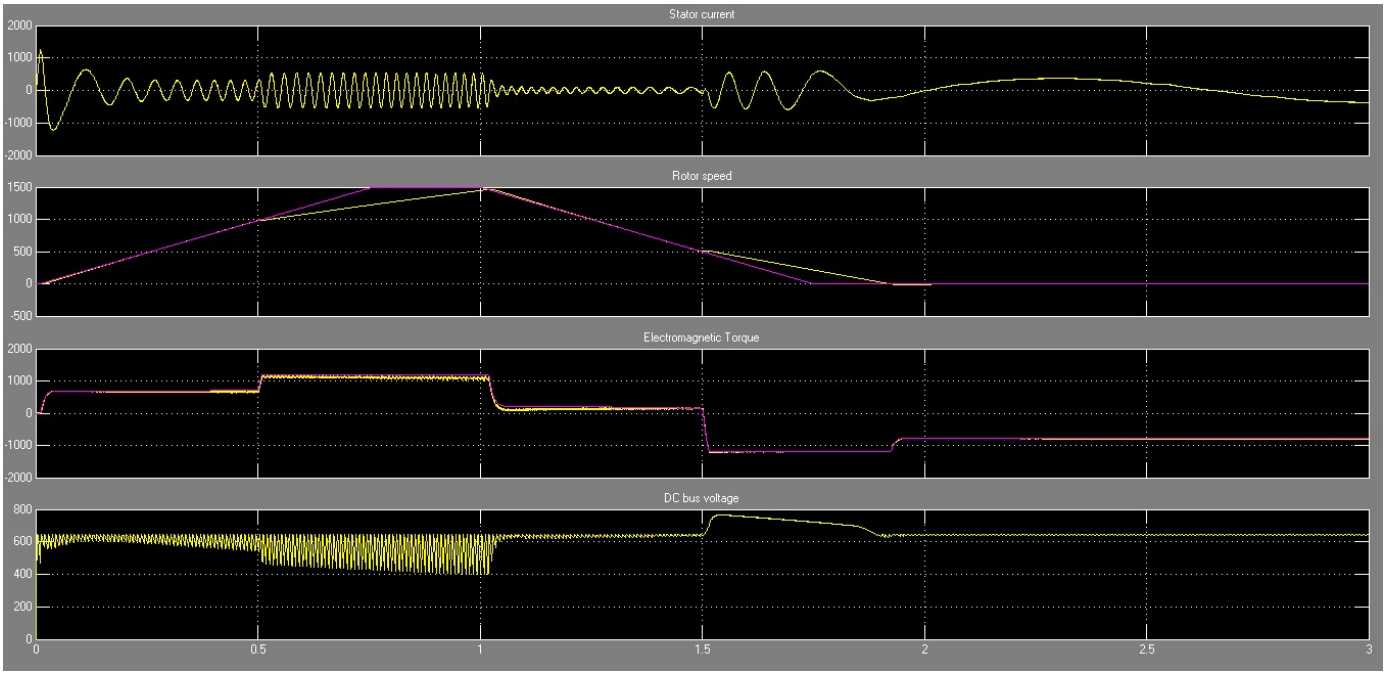

Figure 14. Changes in the stator current, rotation speed and electromagnetic moment of the electric motor and DC bus voltage of the direct current medium of the inverter FLIRT 3 for $\omega_r = 1500$ rpm and $T_m = \pm 792$ Nm.

The results shown in **Figure 14** were obtained after a number of running simulations with the initial conditions specified above. The version number of the software MATLAB-Simulink is 2013a (8.1.0.604, win 64, License Number: 8746166).

The simulation results show that the acceleration of the train up to t = 0.5 s is achieved with a constant electromagnetic moment on the electric motor shaft of $T_e = 810$ Nm, and when the load on the electric motor increased, the electromagnetic moment also increased to $T_e = 1050$ Nm. The speed of the electric motor $\omega_r = 1500$ rpm (v = 90 km/h) is reached at the moment t = 1 when braking starts until t = 1.75 s when the electric multiple unit stops. It is interesting to note that the speed of $\omega_r = 1500$ rpm is not reached before t = 1 s and if the limiters allow it even earlier. The rotating electromagnetic torque on the electric motor shaft is very small during braking in the interval from t = 1–1.5 s because the motor brakes due to the drag resistance of $T_m = +792$ Nm, and from t > 1.5 s a negative (braking) electromagnetic is generated the moment that overcomes the inertial drag resistance of $T_m = -792$ Nm, bringing the train to rest.

With these input parameters, the stator current of the electric motor does not exceed 1000 A, and the DC bus voltage is 800 V.

If the same input parameters of the system as in the previous example are assumed, but now with a new set speed of the electric motor of $\omega_r = 500$ rpm (v = 30 km/h), the change in the output values is shown in **Figure 15** (such conditions exist when the train driver wants to accelerate the train more slowly with the same traction resistances as in the previous example, but up to the train speed limit of v = 30 km/h).

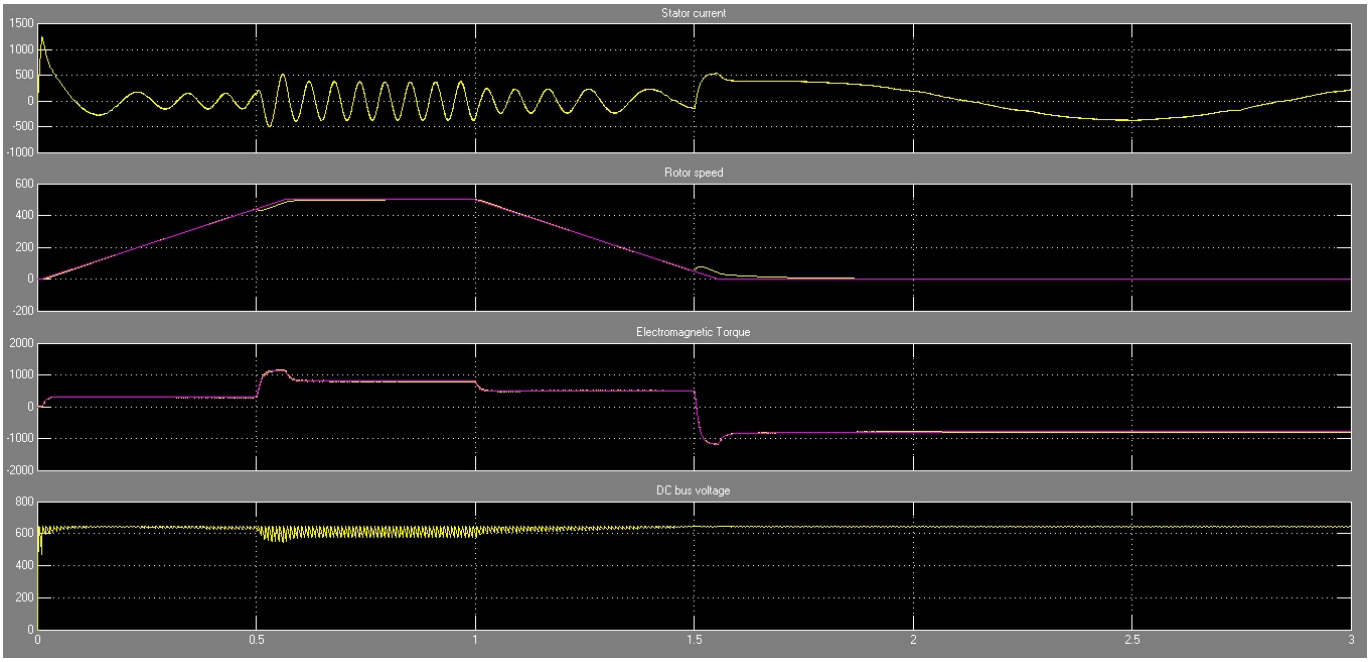

Figure 15. Changes in the stator current, rotation speed and electromagnetic moment of the electric motor and DC bus voltage of the direct current medium of the inverter FLIRT 3 for $\omega_r = 500$ rpm and $T_m = \pm 792$ Nm.

The results shown in **Figure 15** were obtained after a number of running simulations with the initial conditions specified above.

In this case, the starting of the electric motor from rest is done with a smaller electromagnetic moment $T_e = 200$ Nm until the moment t = 0.5 s when the electric motor is loaded with $T_m = 792$ Nm and increases to the value $T_e = 810$ Nm.

The set speed of $\omega_r = 500$ rpm (v = 30 km/h) is reached at the moment t = 0.6 s and is maintained until the moment t = 1 s when the start of braking is set. Braking starts with an electromagnetic torque T_e smaller than the positive resistive torque of $T_m = +792$ Nm and lasts until a complete stop at the moment t = 1.5 s. For $t > 1.5$ s the electric motor remains braked due to the generation of a negative electromagnetic moment T_e that overcomes the negative resistance of $T_m = -792$ Nm.

With these input parameters, the stator current of the electric motor does not exceed 600 A, and the DC bus voltage is 620 V.

Numerous simulations with the specified input parameters, but now with variable and permitted contact network voltage values of 19.5–27.5 kV and a total voltage distortion equal to or less than 8% (the European Standard SRPS EN 50162:2010), show the same or approximately the same change in output values as in **Figures 14** and **15**.

This fact indicates a very important feature of the fast, light, innovative regional train "FLIRT 3", which is that the train's electric traction drive has completely eliminated the influence of the contact network voltage. Due to the mentioned fact, it can be concluded that these electric multiple units represent a good driving railway solution.

The presented simulation results are fully confirmed with the experimental results presented in the literature [1].

It should be noted that the described MATLAB-Simulink model of the operation

simulation of the fast, light, innovative regional train “FLIRT 3” in the traction and braking mode enables the analysis of numerous other initial operating conditions related to the changing conditions of the train's power supply from the contact network, i.e., to changing conditions of the mechanical load of the train.

The described model enables the monitoring of changes in stator current, speed, and electromagnetic torque of traction motors for different permitted values and distortions of contact network voltage as well as for different mechanical loads during FLIRT 3 movement speed regulation.

4. Conclusion

The described simulation model completely objectively depicts the operation of the fast, light, innovative regional train “FLIRT 3” in traction and braking mode. The model made it possible to observe the electrical and mechanical parameters of the drive three-phase asynchronous motors for different permissible voltage values and voltage distortions at the point of connection of the multiple power unit to the contact network, different mechanical loads, and different rotation speeds of traction electric motors.

The described model enables the monitoring of changes in stator current, speed, and electromagnetic torque of traction motors for: different permitted values and distortions of contact network voltage as well as for different mechanical loads during FLIRT 3 movement speed regulation.

Numerous simulations show a very important feature of the electric multiple unit of the fast, light, innovative regional train “FLIRT 3”, which is that the vehicle's automatic regulation system has completely eliminated the influence of changing voltage value and voltage distortion in the contact network on the vehicle's operation. This stability of the drive to changes in voltage value and voltage distortion in the contact network is very important in the exploitation of railway electric traction vehicles and represents a special quality of this electric multiple unit.

The results of the simulations were fully confirmed by the experimental measurements performed at the fast, light, innovative regional train “FLIRT 3”.

Author contributions: Conceptualization, BG and VAB; methodology, BG; software, BG; validation, BG and VAB; formal analysis, BG and VAB; investigation, BG; resources, BG; data curation, BG; writing—original draft preparation, BG; writing—review and editing, BG; visualization, BG; supervision, BG; project administration, BG; funding acquisition, BG. All authors have read and agreed to the published version of the manuscript.

Conflict of interest: The authors declare no conflict of interest.

References

1. Stadler. Train Description- L-4547 Flirt 3 EMU Serbia. Document No PR_5382875. Stadler; 2023.
2. Gavrilovic B, Bundalo Z, Blagojevic Z. Regenerative braking of electric multiple unit serie 413/417 of joint stock company for passenger railway transport, Serbia Voz. In: Proceedings of the18th International Symposium INFOTEH-JAHORINA; 20-22 March 2019; Jahorina, Bosnia and Herzegovina.
3. Bose BK. Modern Power Electronics and AC Drives. Prentice-Hall; 2002.

4. Grelet G, Clerc G. Electric Actuators (French). Éditions Eyrolles, Paris; 1997.
5. Krause PC. Analysis of Electric Machinery. McGraw-Hill; 1986.
6. Gavrilovic BS. Research and Analysis in the Electric Traction System of the Serbian Railways. Eliva Press; 2023.
7. Boldea I, Nasar SA. Nasar: Electric Drives, 3rd ed. CRC Press; 2017.
8. Nondahl TA. Microprocessor Control of Motor Drives and Power Converters. IEEE Industry Application Society; 1993.
9. Bolton W. Mechatronics: Electronic Control Systems in Mechanical and Electrical Engineering, 3rd ed. Pearson Education; 2004.
10. Kaur H. Electric Drives and Their Controlling Techniques, 1st ed. Scholar's Press London; 2019.
11. Mohan N, Raju S. Analysis and Control of Electric Drives: Simulations and Laboratory Implementation. John Wiley & Sons; 2021.
12. Merabet A (editor). Advanced Control Systems for Electric Drives. MDPI; 2020.
13. Dorji C. Review of Electric Motor Drives. Available online: https://www.researchgate.net/profile/Cheku-Dorji-3/publication/282249201_REVIEW_OF_ELECTRIC_DRIVES/links/5a2657a80f7e9b71dd0a043f/REVIEW-OF-ELECTRIC-DRIVES.pdf (accessed on 12 November 2023).
14. Golnaraghi F, Kuo BC. Automatic Control Systems, 9th ed. John Wiley & Sons; 2010.
15. Kryukov OV, Blagodarov DA, Dulnev NN, et al. Intelligent Control of Electric Machine Drive Systems. 2018 X International Conference on Electrical Power Drive Systems (ICEPDS); 3-6 October 2018; Novocherkassk, Russia. pp. 1-4. doi: 10.1109/icepds.2018.8571670
16. Hughes A. Electric Motors and Drives—Fundamentals. In: Types and Applications, 3rd ed. Elsevier; 2006.
17. Schröder D. Electric Drives—Basics (German). Springer Berlin Heidelberg; 2007. doi: 10.1007/978-3-540-73005-7
18. Jauch C, Tamilarasan S, Bovee K, et al. Modeling for drivability and drivability improving control of HEV. Control Engineering Practice. 2018; 70: 50-62. doi: 10.1016/j.conengprac.2017.09.014
19. Brkić R, Adamović Ž, Bukvić M. Modeling of reliability and availability of data transmission in railway system. Advanced Engineering Letters. 2022; 1(4). doi: 10.46793/adeletters.2022.1.4.3
20. Hidirov S, Guler H. Reliability, availability and maintainability analyses for railway infrastructure management. Structure and Infrastructure Engineering. 2019; 15(9): 1221-1233. doi: 10.1080/15732479.2019.1615964
21. Mosayyebi M, Shakibian H, Azmi R. Statistical and Reliability Analysis of the Iran Railway System as a Complex Network. International Journal of Web Research. 2022; 5(1). doi: 10.22133/ijwr.2022.346545.1121
22. Adamović Ž, Josimović L. Technical Diagnostics. Society for Technical Diagnostics of Serbia; 2020.